ORIGINAL ARTICLE
https://doi.org/10.4046/trd.2020.0107
ISSN: 1738-3536(Print)/2005-6184(Online) • Tuberc Respir Dis 2021;84:55-66

trd Tuberculosis & Respiratory Diseases

Effects of Particulate Matter 10 Inhalation on Lung Tissue RNA expression in a Murine Model

Heejae Han, M.S.[1], Eun-Yi Oh, M.S.[2], Jae-Hyun Lee, M.S.[2,3], Jung-Won Park, M.S.[2,3] and Hye Jung Park, M.D., Ph.D.[1]

[1]Department of Internal Medicine, Gangnam Severance Hospital, Seoul, [2]Institute of Allergy, Yonsei University College of Medicine, Seoul, [3]Division of Allergy and Immunology, Department of Internal Medicine, Yonsei University College of Medicine, Seoul, Republic of Korea

Background: Particulate matter 10 (PM_{10}; airborne particles <10 μm) inhalation has been demonstrated to induce airway and lung diseases. In this study, we investigate the effects of PM_{10} inhalation on RNA expression in lung tissues using a murine model.

Methods: Female BALB/c mice were affected with PM_{10}, ovalbumin (OVA), or both OVA and PM_{10}. PM_{10} was administered intranasally while OVA was both intraperitoneally injected and intranasally administered. Treatments occurred 4 times over a 2-week period. Two days after the final challenges, mice were sacrificed. Full RNA sequencing using lung homogenates was conducted.

Results: While PM_{10} did not induce cell proliferation in bronchoalveolar fluid or lead to airway hyper-responsiveness, it did cause airway inflammation and lung fibrosis. Levels of interleukin 1β, tumor necrosis factor-α, and transforming growth factor-β in lung homogenates were significantly elevated in the PM_{10}-treated group, compared to the control group. The PM_{10} group also showed increased RNA expression of *Rn45a*, *Snord22*, *Atp6v0c-ps2*, *Snora28*, *Snord15b*, *Snora70*, and *Mmp12*. Generally, genes associated with RNA splicing, DNA repair, the inflammatory response, the immune response, cell death, and apoptotic processes were highly expressed in the PM_{10}-treated group. The OVA/PM_{10} treatment did not produce greater effects than OVA alone. However, the OVA/PM_{10}-treated group did show increased RNA expression of *Clca1*, *Snord22*, *Retnla*, *Prg2*, *Tff2*, *Atp6v0c-ps2*, and *Fcgbp* when compared to the control groups. These genes are associated with RNA splicing, DNA repair, the inflammatory response, and the immune response.

Conclusion: Inhalation of PM_{10} extensively altered RNA expression while also inducing cellular inflammation, fibrosis, and increased inflammatory cytokines in this murine mouse model.

Keywords: Particulate Matter; RNA Sequencing; Lung

Address for correspondence: Hye Jung Park, M.D., Ph.D.
Division of Pulmonology, Department of Internal Medicine, Gangnam Severance Hospital, Yonsei University College of Medicine, 211 Eonju-ro, Gangnam-gu, Seoul 06273, Republic of Korea
Phone: 82-2-2019-3302, **Fax:** 82-2-3463-3882, **E-mail:** craft7820@yuhs.ac
Received: Sep. 15, 2020, **Revised:** Oct. 21, 2020, **Accepted:** Nov. 30, 2020, **Published online:** Nov. 30, 2020

Introduction

Air pollution is an important problem worldwide, and it certainly has negative effects on general health[1-3]. Particulate matter 10 (<10 μm; PM_{10}) is a one of the major components of air pollution. It includes high levels of elements such as silicon, barium, aluminum, zinc, copper, and lead[4,5]. PM_{10} enters the airway through the nose and mouth, and as a result it can potentially cause injury to the respiratory tract, including the trachea, bronchus, alveoli, and even lung parenchyma. Studies have also indicated that chronic and intensive inhalation of PM_{10} can induce and enhance airway and lung diseases. For example, epidemiologic data have shown that asthma can be developed and aggravated by ambient pollutants like PM_{10}[6-8], and chronic obstructive pulmonary disease (COPD) is also sensitive to PM_{10} exposure[9-12].

Some indications of the mechanisms underlying these effects have been found[13]. For example, innate and adaptive immune responses in the airway and lung can be altered by extrinsic irritants in general[14], and PM_{10} exposure can alter mechanical and immunological barriers in airway disease[15]. At the molecular level, evidence indicates that interleukin (IL)-1β, IL-6, NOD-like receptor pyrin domain-containning protein 3, and chemokine (C-C motif) ligand 20 may be key mediators of the effects of PM_{10} on airway and lung tissue[16-18]. However, PM_{10} particles are extremely small and consist of variable elements. We therefore hypothesized that PM_{10} can alter RNA expression in extensive range, potentially leading to visible inflammation and other side effects. Elucidating the patterns of RNA expression changes in response to PM_{10} in a murine model may be helpful for predicting its effects on human health.

Materials and Methods

1. Animal model designs

Female BALB/c mice, between 5 and 6 weeks old (Orient, Daejeon, Korea), were maintained at conventional animal facilities under pathogen-free conditions, and five mice were assigned in each group. To establish the PM_{10}-induced murine model (PM_{10} model), PM_{10} (ERMCZ-120 certified reference material; Sigma-Aldrich, St. Louis, MO, USA; 100 μg [PM100] or 200 μg [PM200]) suspended in 20 μL normal saline was intranasally administered four times over 2 weeks. To establish the ovalbumin (OVA)-induced asthma murine model (OVA model), mice were sensitized with 20 μg OVA (Sigma-Aldrich)

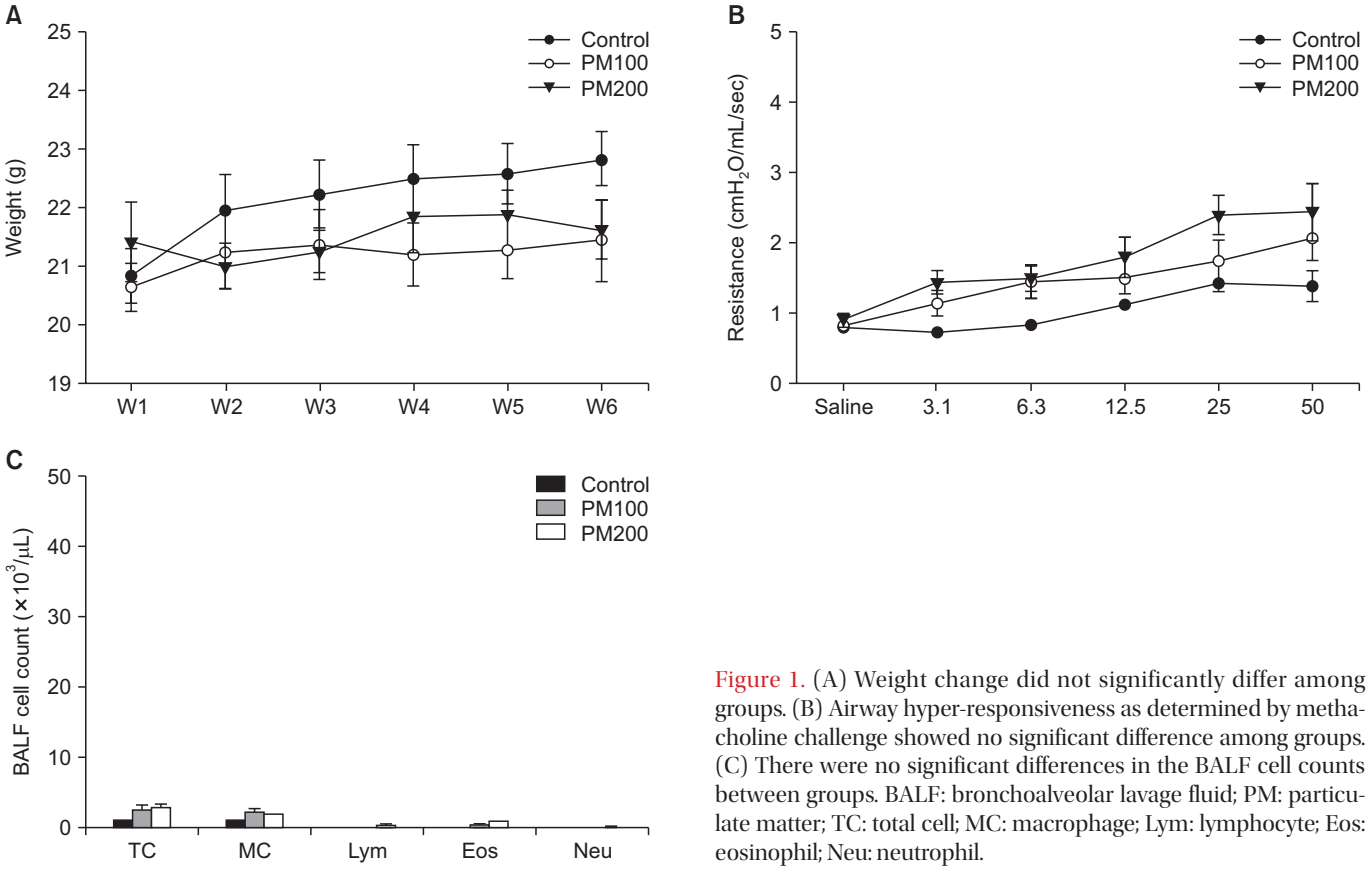

Figure 1. (A) Weight change did not significantly differ among groups. (B) Airway hyper-responsiveness as determined by methacholine challenge showed no significant difference among groups. (C) There were no significant differences in the BALF cell counts between groups. BALF: bronchoalveolar lavage fluid; PM: particulate matter; TC: total cell; MC: macrophage; Lym: lymphocyte; Eos: eosinophil; Neu: neutrophil.

suspended in 1% aluminum hydroxide (Resorptar; Indergen, New York, NY, USA) by intraperitoneal injection on days 1 and 14. On days 21, 22, and 23, the OVA-sensitized mice were challenged intranasally with 30 μL of OVA (1 mg/mL) in saline solution. An OVA/PM_{10}-treated model was established by the above two treatments simultaneously. All mice were sacrificed 2 days after their last treatment (Supplementary Figure S1). All experimental procedures of mice studies were approved by the Institutional Animal Care and Use Committee, Animal Research Ethics Board of Yonsei University (Seoul, Korea) (IACUC approval number, 2020-0087) and were performed in accordance with the Committee's guidelines and regulations for animal care.

2. Measurement of airway hyper-responsiveness

Airway hyper-responsiveness (AHR) to inhaled aerosolized methacholine (MCh; Sigma-Aldrich) was measured using a forced oscillation technique (FlexiVent; SCIREQ, Montreal, QC, Canada) on the sacrifice day, as described in a previous study[19-21]. Aerosolized phosphate-buffered saline or MCh at varying concentrations (3.125 mg/mL, 6.25 mg/mL, 12.5 mg/mL, 25.0 mg/mL, or 50.0 mg/mL), was administered to mice for 10 s via a nebulizer connected to a ventilator. Then, AHR was assessed by measurements of airway resistance.

3. Inflammatory cell counting in bronchoalveolar lavage fluid

To collect bronchoalveolar lavage fluid (BALF), we performed lung lavage, using 1 mL of Hank's balanced salt solution (HBSS) through a tracheal tube. The recovered BALF was centrifuged and resuspended in 300 μL HBSS. Total cell numbers were determined using a hemocytometer and trypan blue staining. BALF cells were centrifuged by cytocentrifugation (Cytospin 3; Thermo Fisher Scientific, Waltham, MA, USA) and were pelleted to cytospin slides. The slides were stained with hematoxylin and eosin (H&E Hemacolor; Merck, Darmstadt, Germany) and a differential count of inflammatory cells was performed (200 cells per slide).

4. Histological analysis

The lung that was not used for BALF collection was fixed in 4% formalin and embedded in paraffin. Lung sections were cut into 3–4-μm-thick slices and stained with H&E, periodic acid-Schiff, and Masson trichrome (M&T) for histological analysis. The slides were observed under a light microscope (×200 magnification). Fibrosis area was measured by estimating the color-pixel count over the pre-set threshold color on M&T-stained slides at ×200 magnification using MetaMorph program (Molecular Devices, Sunnyvale, CA, USA).

5. Lung homogenate

After collecting BALF, remaining lung tissue was resected and homogenized using a tissue homogenizer (Biospec Products, Bartlesville, OK, USA) in lysis buffer and protease inhibitor solution (Sigma-Aldrich). After incubation and centrifugation, supernatants were harvested and passed through a

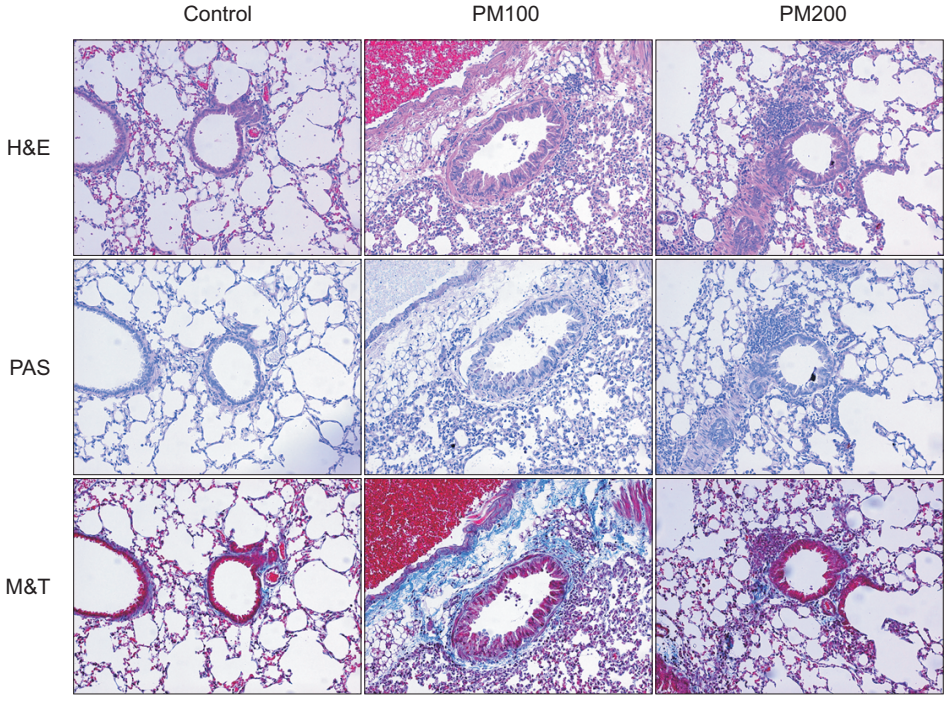

Figure 2. Pathological analysis revealed PM_{10} treatment led to airway inflammation and lung fibrosis (H&E, PAS, and M&T; ×200). H&E: hematoxylin and eosin; PAS: periodic acid-Schiff; PM: particulate matter; M&T: Masson trichrome.

0.45-micron filter (Gelman Science, Ann Arbor, MI, USA). The final preparations were stored at –20°C for cytokine analysis as described previously[19].

6. Analysis of cytokines

Concentrations of interleukin (IL)-1β, tumor necrosis factor-α (TNF-α), IL-13, and transforming growth factor-β (TGF-β) in lung homogenates were assessed by enzyme-linked immunosorbent assay (R&D Systems, San Diego, CA, USA) according to the manufacturer's instructions. All samples were assessed in duplicate.

7. Full RNA sequencing

Total RNA was extracted from lung tissue using Trizol reagent (Invitrogen, Carlsbad, CA, USA). The isolated mRNAs were used for cDNA synthesis. Libraries were prepared using the NEBNext Ultra II Directional RNA Seq Kit (New England BioLabs, Inc., Hitchin, UK). Indexing was performed using the Illumina indexes 1–12. The enrichment step was carried out using polymerase chain reaction (PCR). Subsequently, libraries were checked using the Agilent 2100 bioanalyzer (Agilent Technologies, Amstelveen, The Netherlands), to evaluate the mean fragment size. Quantification was performed using the library quantification kit with an ND 2000 Spectrophotometer (Thermo Fisher Scientific) and StepOne Real Time PCR System (Life Technologies, Inc., Carlsbad, CA, USA). High-throughput sequencing was performed as paired end 100 sequencing using NovaSeq 6000 (Illumina, Inc., San Diego, CA, USA).

Quality control of raw sequencing data was performed using FastQC (Simon, 2010). The results of fast QC are presented in Supplementary Figure S2. Adapter and low-quality reads (<Q20) were removed using FASTX_Trimmer (Hannon Lab, 2014) and BBMap (Bushnell, 2014). Then, the trimmed reads were mapped to the reference genome using TopHat[22]. Gene expression levels were estimated by calculating fragments per kb per million reads (FPKM) using Cufflinks[23]. The FPKM values were normalized based on a quantile normalization method using EdgeR within R (R development Core Team, 2016). Data mining and graphic visualization including define upregulated or downregulated gene expression were performed using ExDEGA (E-Biogen, Inc., Seoul, Korea).

8. Statistical analysis

All results are expressed as the mean±standard error. The AHR data were analyzed using repeated-measure analysis of variance (ANOVA), followed by a *post-hoc* Bonferroni test. One-way ANOVA was performed to assess the significance of differences in BALF cell count, cytokine levels, and quantitative fibrosis among groups. All statistical analyses were performed with IBM SPSS version 18.0 (SPSS Inc., Chicago, IL, USA). p-values <0.05 were considered statistically significant.

Results

1. Comparison of weight changes, AHR, and BALF between control and PM_{10}-treated groups

All mice increased in weight over the course of the experiment. There was a non-significant trend for the PM_{10}-treated group (PM100 and PM200) to gain less weight (Figure 1A). AHR obtained by MCh challenge showed no significant changes among the three groups (Figure 1B). BALF cell counts were also not significantly different among groups (Figure 1C).

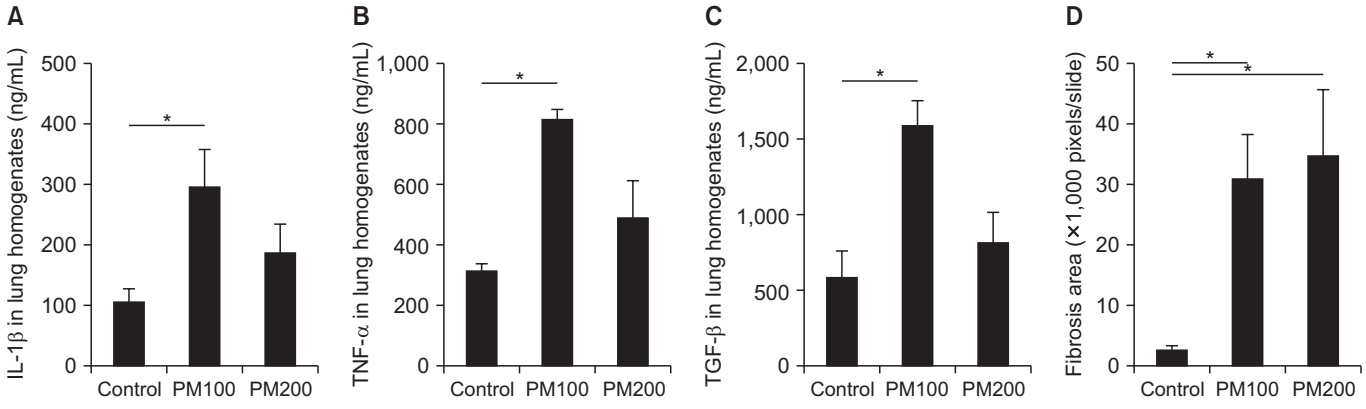

Figure 3. IL-1β (A), TNF-α (B), and TGF-β (C) levels in lung homogenates were significantly higher in the PM100-treated group compared to the control group. Quantitative fibrosis was significant and severe in the PM_{10}-treated group compared to the control group (D). IL-1β: interleukin 1β; PM: particulate matter; TNF-α: tumor necrosis factor-α; TGF-β: transforming growth factor-β. *p<0.05.

A

	Fold change (PM_{10} vs. control)	Normalized data (log_2) Control	Normalized data (log_2) PM_{10}
Rn45s	8,058.365	0.046	13.023
Snord22	675.879	0.046	9.446
Atp6v0c-ps2	194.596	0.048	7.653
Snora28	84.314	0.040	6.437
Snord15b	78.076	0.039	6.326
Snora70	70.963	0.038	6.187
Mmp12	56.102	1.246	7.056
Rprl3	51.286	0.036	5.717
Bc1	42.404	0.034	5.440
Snora17	31.237	0.031	4.997
AA467197	27.239	0.818	5.586
Snora26	26.538	0.030	4.760
Ccl17	19.585	3.338	7.630
Rpph1	19.420	1.865	6.144
Clec4d	18.464	1.815	6.021
≈	≈	≈	≈
Lce3a	0.004	8.049	0.000
Mylpf	0.004	9.441	1.341
Tnnt3	0.003	9.394	1.204
Serpinb12	0.003	8.326	0.000
Crct1	0.003	8.528	0.000
Lgals7	0.003	8.740	0.182
Serpinb3c	0.002	9.134	0.000
Mt4 (metallothionecin 4)	0.002	9.233	0.000
Acta1	0.001	9.954	0.000
Tnnc2	0.001	9.988	0.000
Krt4 (keratin 4)	0.001	10.232	0.226
Sprr2a3	0.001	10.174	0.000
Krtdap	0.001	10.466	0.000
Krt13 (keratin 13)	0.000	11.368	0.000
Chil4 (chitinase-like 4)	0.000	11.664	0.091

B

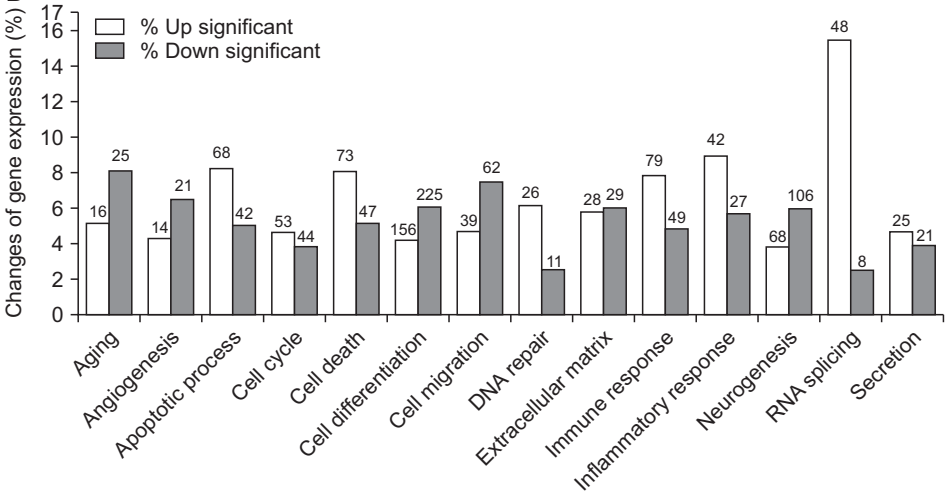

Figure 4. (A) Genes showing the largest difference between the control and PM_{10}-treated groups. (B) RNA expression of genes associated with RNA splicing, DNA repair, the inflammatory response, the immune response, cell death, and apoptotic process were increased in the PM_{10}-treated group compared to the control group. The number of genes with significant change are presented at the top of bar. PM: particulate matter.

https://doi.org/10.4046/trd.2020.0107

2. Comparison of pathologic findings between control and PM_{10}-treated groups

Compared to the control group, the PM_{10}-treated group (PM100 and PM200) showed cellular infiltration in the airway and lung parenchyme. Airway wall thickness, goblet cell hyperplasia, and inflammatory cellular proliferation were observed predominantly in the PM_{10}-treated group. In addition, fibrosis in lung parenchyme and peribronchial tissues were also predominant in the PM_{10}-treated group, compared to the control group (Figure 2).

3. Comparison of cytokine levels in lung homogenates and quantitative fibrosis between the control and PM_{10}-treated groups

The levels of IL-1β, TNF-α, and TGF-β in lung homogenates were higher in the PM_{10}-treated group than in the control group, but statistical significance was observed only for the PM100 group (Figure 3A–C). As evidence by the results of the fibrosis-area analysis, PM_{10} induced significant lung fibrosis (Figure 3D).

4. Comparison of RNA expression between the control and PM_{10}-treated groups

The PM_{10} model showed increased RNA expression of *Rn45a*, *Snord22* (small nucleolar RNA), *Atp6v0c-ps2* (ATPase, H+ transporting, lysosomal V0 subunit C, pseudogene 2), *Snora28*, *Snord15b*, *Snora70*, and *Mmp12* compared to control group (Figure 4A). Generally, genes associated with RNA splicing, DNA repair, inflammatory response, immune response, cell death, and the apoptotic process were highly expressed in the PM_{10} model compared to control group (Figure 4B).

5. Comparison of weight changes, airway hyperresponsiveness, and BALF cell count between the control, OVA, and OVA/PM_{10}-treated groups

All mice increased in weight over the course of the experiment. Among all the groups, the final weight of the control group was the heaviest (Figure 5A). AHR obtained by MCh challenge in both OVA-treated groups (OVA and OVA/PM_{10}) was predominant compared to the control group. However, it was not significantly different between the OVA and OVA/PM_{10}-treated groups (Figure 5B). Total cell, macrophage, and

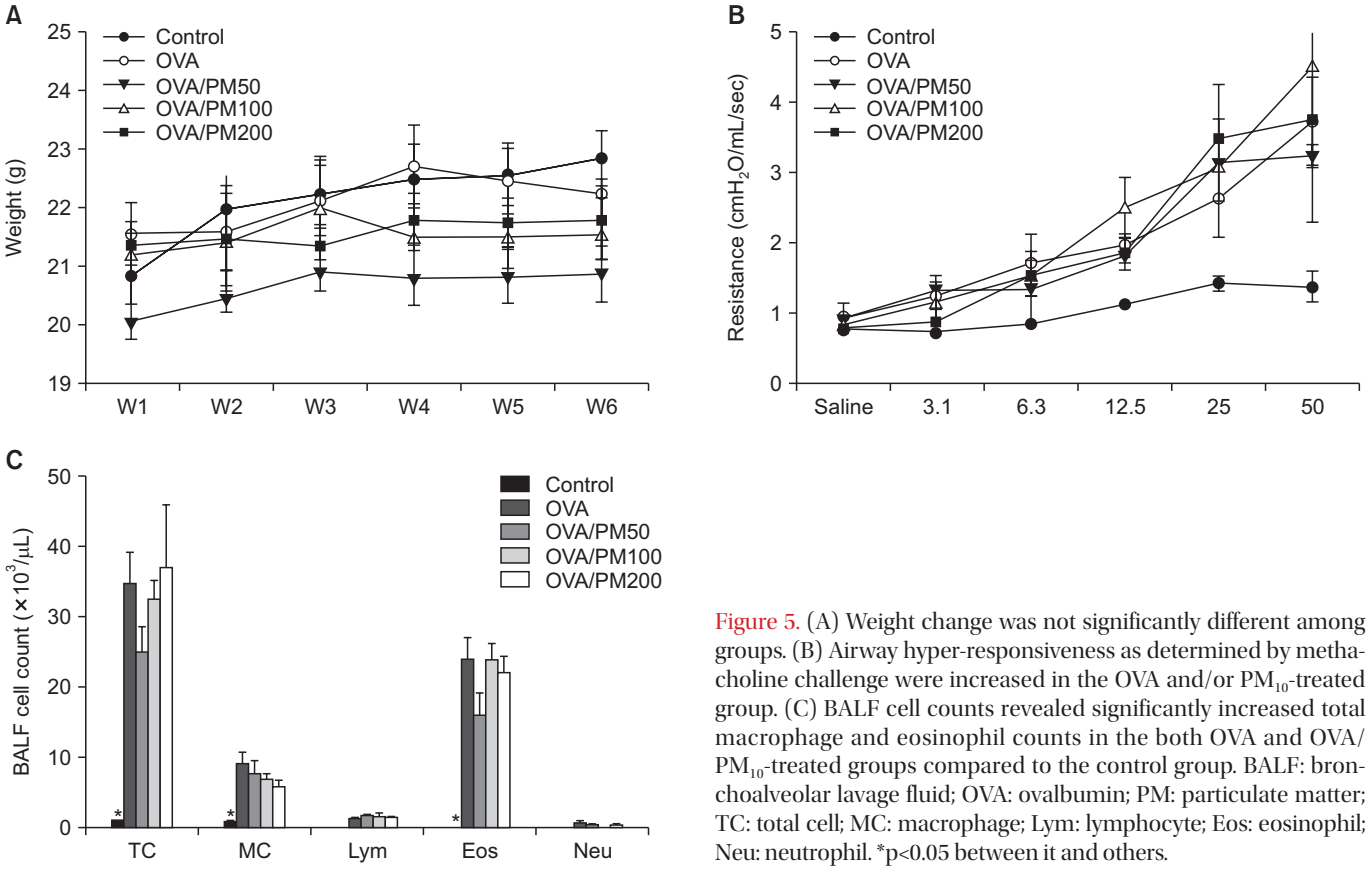

Figure 5. (A) Weight change was not significantly different among groups. (B) Airway hyper-responsiveness as determined by methacholine challenge were increased in the OVA and/or PM_{10}-treated group. (C) BALF cell counts revealed significantly increased total macrophage and eosinophil counts in the both OVA and OVA/PM_{10}-treated groups compared to the control group. BALF: bronchoalveolar lavage fluid; OVA: ovalbumin; PM: particulate matter; TC: total cell; MC: macrophage; Lym: lymphocyte; Eos: eosinophil; Neu: neutrophil. *p<0.05 between it and others.

eosinophil counts in BALF were highly elevated in all OVA-treated groups compared with the control group. However, they were not significantly different between the OVA and OVA/PM_{10}-treated groups (Figure 5C).

6. Comparison of pathologic findings between control, OVA, and OVA/PM_{10}-treated group

All OVA-treated groups showed prominent inflammatory cell proliferation and fibrosis in airway, peribronchial tissue, and lung parenchyme, compared to control group. However, treatment of OVA/PM_{10} did not have additive effect on OVA alone (Figure 6).

7. Comparison of cytokine levels in lung homogenates and quantitative fibrosis between in control, OVA, and OVA/PM_{10}-treated group

The levels of IL-1β, TNF-α, IL-13, and TGF-β in lung homogenates were increased in the OVA-treated group. However, the effects of OVA/PM_{10} treatment were not greater than those of OVA alone (Figure 7A–D). Both OVA and OVA/PM_{10} treatment induced significant lung fibrosis as evident in fibrosis-are analysis; however, OVA/PM_{10} treatment were not greater than those of OVA alone (Figure 7E).

8. Comparison of RNA expression between the control and OVA/PM_{10}-treated groups

The OVA/PM_{10}-treated model showed increased RNA expression of *Clca1* (chloride channel accessory 1), *Snord22*, *Retnla* (resistin like alpha), *Prg2* (proteoglycan 2, bone marrow), *Tff2* (trefoil factor 2), *Atp6v0c-ps2*, and *Fcgbp* (Fc fragment of IgG binding protein) compared to the control (Figure 8A). Overall, this model showed increased RNA expression of genes associated with RNA splicing, DNA repair, inflammatory response, and immune response compared to control group (Figure 8B).

Discussion

This study confirmed that PM_{10} can alter immune and inflammatory processes of the lung at the gene, protein, and cellular levels, using a murine model. In a substantial advance on previous work, we showed that exposure to PM_{10} can extensively alter RNA expression in lung homogenates. PM_{10} induced increased RNA expression associated with RNA splicing, DNA repair, cell death, apoptotic processes, the inflammatory response, and the immune response. The above processes are associated with the cell cycle, cell viability, and cellular proliferation. Potential consequences of such widely altered RNA expression profiles include necrosis, malignancy, and other diseases. Referring to the results of our RNA expression analysis, we can potentially predict various clinical effects

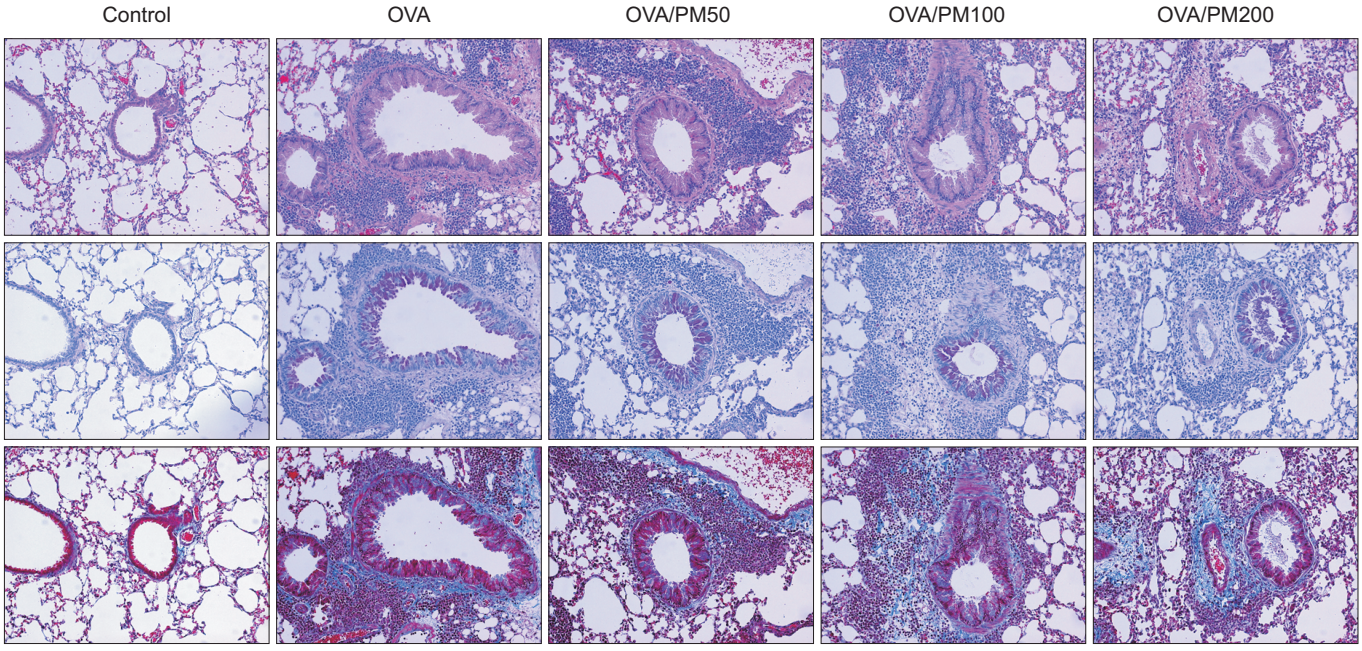

Figure 6. Pathological findings revealed that both the OVA and OVA/PM_{10} treatments led to airway inflammation and lung fibrosis (H&E, PAS, and M&T; all ×200). H&E: hematoxylin and eosin; OVA: ovalbumin; PAS: periodic acid-Schiff; PM: particulate matter; M&T: Masson trichrome.

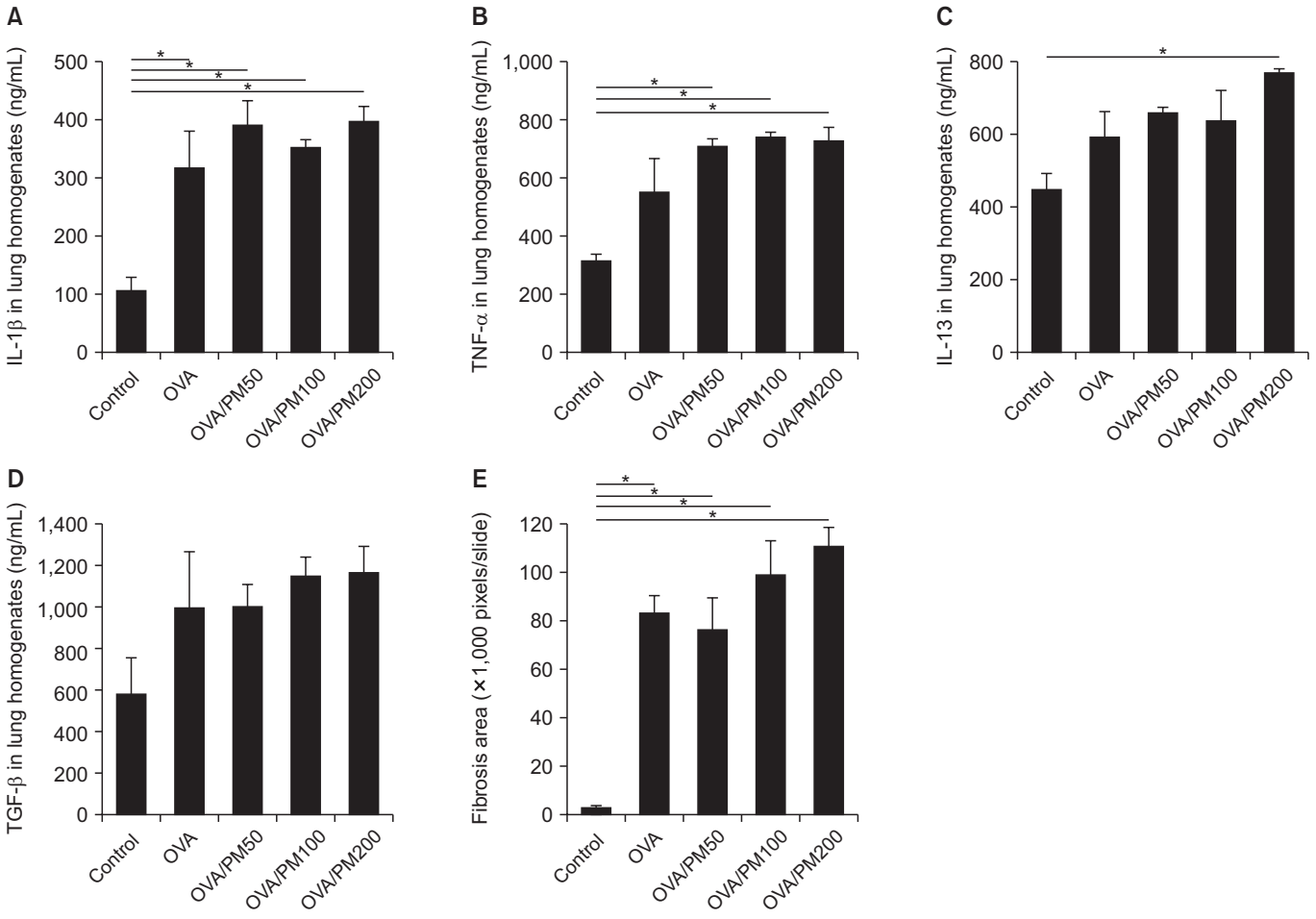

Figure 7. IL-1β (A), TNF-α (B), IL-13 (C), and TGF-β (D) levels in lung homogenates were increased in the OVA and OVA/PM_{10}-treated groups. Quantitative fibrosis was significant and severe in the OVA and OVA/PM_{10}-treated groups compared to the control group (E). IL: interleukin; OVA: ovalbumin; PM: particulate matter; TNF-α: tumor necrosis factor-α; TGF-β: transforming growth factor-β. *p<0.05.

of PM_{10}, and conduct further studies concerning mechanisms underlying these effects.

Inhalation of PM_{10} induced proliferation of inflammatory cells and fibrosis in peri-bronchial and lung tissue. We speculated that abundant helper T cell type I (Th1) type inflammatory cytokines increased in lung homogenates might lead to these changes. Some previous studies have shown similar results: Th1 type inflammatory cytokines increased in PM_{10} treated model[24,25]. Other studies also showed PM_{10} is associated with inflammation[26] or fibrosis[27] of lung. Based on this study and previous *in vitro* and *in vivo* studies, PM_{10} is definitely toxic material to airway and lung parenchyme. Many human studies also support that PM_{10} has negative effects on lung and airway diseases[28].

It is notable that we observed extremely high expression of *Rn45s* (8,058-fold change), *Snord22* (676-fold change), and *Atp6v0c-ps2* (196-fold change) in the PM_{10} treated group, compared to the control group. Rn45s is known to be associated with RNA toxicity, but its function has not been fully elucidated[29]. Snord22 is small nucleolar RNA. *Atp6v0c-ps2* is associated with ATPase, H+ transporting, and lysosomal V0 subunit C. This plays a central role in H(+) transport across cellular membranes[30]. In addition, *Snora28*, *Snord15b*, *Snora70*, *Mmp12*, *Rprl3*, *BC1*, *Snora17*, *AA467197*, *Snora26*, *Ccl17*, *Rpph1*, and *Clec4d* were also highly expressed in the PM_{10}-treated group compared to the control group. These genes are associated with small nucleolar RNA, brain cytoplasmic RNA, or specific chemokines[31,32]. In the OVA/PM_{10}-treated group, the genes *Clca1*, *Snord22*, *Retnla*, *Prg2*, *Tff2*, *Atp6v0c-ps2*, *Fcgbp*, *Muc5ac*, *Itln1*, *Ngp* (neutrophilic granule protein), *Fxyd4* (FXYD domain-containing ion transport regulator 4), *Mzb1* (marginal zone B and B1 cell-specific protein 1), *Mmp12* (matric metallopeptidase 12), *Camp* (cathelicidin antimicrobial peptide), and *Tff1* were upregulated compared to control group.

Some genes were extremely suppressed in the PM_{10}-treated

A

	Fold change (OVA/PM_{10} vs. control)	Normalized data (log_2) Control	Normalized data (log_2) OVA/PM_{10}
Clca1	3,235.352	12.464	0.804
Snord22	203.758	7.716	0.046
Retnla	149.163	15.198	7.978
Prg2	91.784	7.591	1.071
Tff2	70.658	8.905	2.763
Atp6v0c-ps2	67.243	6.120	0.048
Fcgbp	59.644	6.875	0.977
Muc5ac (mucine 5AC)	58.342	5.978	0.111
Itln1 (intelectin 1)	49.599	5.974	0.342
Ngp	45.142	7.168	1.671
Fxyd4	43.610	5.658	0.212
Mzb1	42.705	8.722	3.305
Mmp12	38.894	6.528	1.246
Camp	37.851	6.829	1.587
Tff1 (trefoil factor 1)	33.365	5.093	0.033
≈	≈	≈	≈
Krt6b (keratin 6B)	0.004	8.045	0.126
Serpinb12	0.004	8.326	0.376
Crct1	0.004	8.528	0.561
Mylpf	0.004	9.441	1.463
Lce3b	0.004	7.997	0.006
Defb4	0.004	8.042	0.006
Lce3a	0.004	8.049	0.006
Lgals7	0.003	8.740	0.395
Serpinb3c	0.002	9.134	0.006
Mt4 (metallothionein 4)	0.002	9.233	0.006
Krt4 (keratin 4)	0.001	10.232	0.848
Acta1	0.001	9.954	0.194
Tnnc2	0.001	9.988	0.006
Krtdap	0.001	10.466	0.006
Krt13 (keratin 13)	0.000	11.368	0.153

B

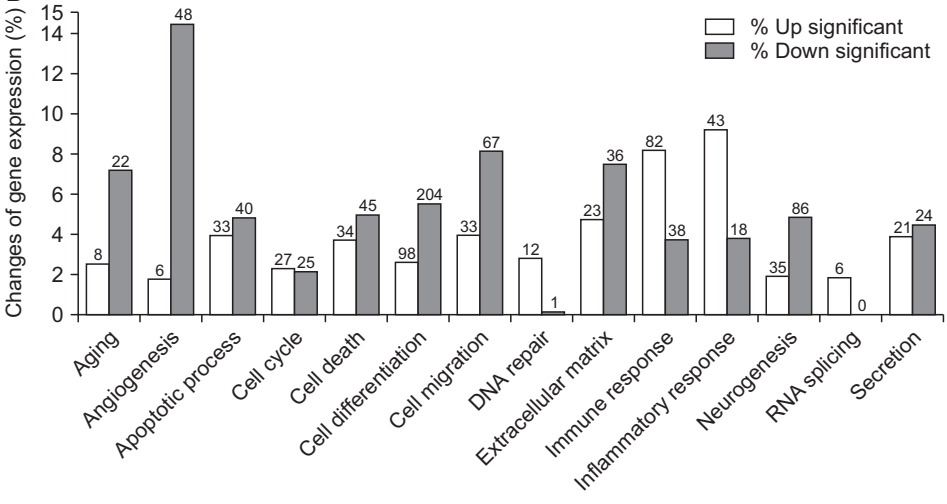

Figure 8. (A) Genes showing the largest difference between the control and OVA/PM_{10}-treated groups. (B) RNA expression of genes associated with RNA splicing, DNA repair, the inflammatory response, and the immune response were increased in the PM_{10}-treated group compared to the control group. The number of genes with significant change are presented at the top of bar. OVA: ovalbumin; PM: particulate matter.

https://doi.org/10.4046/trd.2020.0107

group, compared to the control group: *Chil4*, *Krt13*, *Krtdap* (keratinocyte differentiation associated protein), *Sprr2a3* (small proline-rich protein 2A3), *Krt4*, *Tnnc2* (troponin C2, fast), *Acta1* (actin, alpha 1, skeletal muscle), *Mt4*, *Serpinb3c* (serine peptidase inhibitor, clade B, member 3C), *Lgals7* (lectin, galactose binding, soluble 7), *Crct1* (cysteine-rich C-terminal 1), *Serpinb12* (serine peptidase inhibitor, clade B, member 12), *Tnnt3* (troponin T3, skeletal, fast), *Mylpf* (myosin light chain, phosphorylatable, fast skeletal muscle), and *Lce3a* (late cornified envelope 3A). In the OVA/PM_{10}-treated group, the genes *Krt6b*, *serpinb12*, *Crct1*, *Mylpf*, *Lce3b* (late cornified envelope 3B), *Defb4* (defensin beta 4), *Lce3a*, *Lgals7*, *Serpinb3c*, *Mt4*, *Krt4*, *Acta1*, *Tnnc2*, *Krtdap*, and *Krt13* were substantially downregulated compared to the control group.

PM_{10} altered RNA expression in extensive range. It also increased production of inflammatory cytokines. Inflammation and fibrosis were also induced. However, its effects were only slightly greater than those of OVA. We used an acute-OVA model with intraperitoneal OVA sensitization and intranasal OVA challenge. This model also showed extensive changes of RNA expression and abundant inflammation. Because of the magnitude of the changes caused by OVA, additional effects of PM_{10} were not well revealed. In clinics, severe asthma often leads to hide the clinical effects of other underlying disease, like stable COPD[33]. However, Gold et al.[34] showed that PM mediates and augments allergic sensitization and cellular proliferation using a murine model, and Clifford et al.[35] showed that PM_{10} exposure exacerbates various responses to respiratory viral infection, e.g., increased inflammation and impaired lung function. Then, we are not sure whether addictive or synergic effects of PM_{10} in mild or chronic asthma model[36]. In order to further clarify whether PM_{10} has additive or synergic effects on an allergy model, a further-modified OVA model which does not hide the effects of PM_{10}, is needed.

PM_{10} is a major air pollutant, and thus ends up in the human respiratory system where it can facilitate and aggravate allergic sensitization and airway inflammation[17,37]. This also alters defense mechanisms, including innate immunity in the lungs[38]. Thus, respiratory diseases can be developed and aggravated by exposure to PM_{10}. However, studies elucidating the effects of PM_{10} using murine models are rare, and changes of RNA expression induced by PM_{10} have not been well studied. This study used standardized PM_{10} in a murine model, and showed extensive RNA expression changes. Our results can be used to inform future work using PM_{10}-treated murine models, including further investigation of mechanisms underlying the damaging effects of PM_{10} on the airway and lung. Finally, this study will be helpful to search for therapeutic agents in PM_{10}-exposured human airway and lung diseases.

We showed that inhalation of PM_{10} changed RNA expression in extensive range in a murine model. PM_{10} also induced increased production of inflammatory cytokines, cellular proliferation, and fibrosis. In an acute-OVA model, additional effects of PM_{10} were not observed. Our findings suggest PM_{10} can affect various airway and lung diseases.

Authors' Contributions

Conceptualization: Park HJ. Methodology: Han H, Oh EY. Formal analysis: Park HJ, Lee JH, Park JW. Data curation: Park HJ, Lee JH, Park JW. Software: Park HJ, Lee JH, Park JW. Validation: Han H, Oh EY, Park HJ, Lee JH, Park JW. Investigation: Han H, Oh EY, Park HJ, Lee JH, Park JW. Writing - original draft preparation: Park HJ. Writing - review and editing: Park HJ. Approval of final manuscript: all authors.

Conflicts of Interest

No potential conflict of interest relevant to this article was reported.

Funding

This study was supported by a 2019-grant from The Korean Academy of Tuberculosis and Respiratory Diseases.

Supplementary Material

Supplementary material can be found in the journal homepage (http://www.e-trd.org).

Supplementary Figure S1. Animal model design protocol. IN: intranasal treatment; IP: intraperitoneal treatment; OVA: ovalbumin; PM: particulate matter.

Supplementary Figure S2. Fast QC data in control (A), PM_{10}-treated (B), and OVA/PM_{10}-treated group (C). OVA: ovalbumin; PM: particulate matter.

References

1. Dockery DW, Pope CA, Xu X, Spengler JD, Ware JH, Fay ME, et al. An association between air pollution and mortality in six U.S. cities. N Engl J Med 1993;329:1753-9.
2. McCreanor J, Cullinan P, Nieuwenhuijsen MJ, Stewart-Evans J, Malliarou E, Jarup L, et al. Respiratory effects of exposure to diesel traffic in persons with asthma. N Engl J Med 2007;357:2348-58.
3. Kyung SY, Jeong SH. Particulate-matter related respiratory diseases. Tuberc Respir Dis 2020;83:116-21.
4. Yamada E, Funoki S, Abe Y, Umemura S, Yamaguchi D, Fuse Y. Size distribution and characteristics of chemical components in ambient particulate matter. Anal Sci 2005;21:89-94.

5. Kumar RK, Shadie AM, Bucknall MP, Rutlidge H, Garthwaite L, Herbert C, et al. Differential injurious effects of ambient and traffic-derived particulate matter on airway epithelial cells. Respirology 2015;20:73-9.
6. Penard-Morand C, Raherison C, Charpin D, Kopferschmitt C, Lavaud F, Caillaud D, et al. Long-term exposure to close-proximity air pollution and asthma and allergies in urban children. Eur Respir J 2010;36:33-40.
7. Jacquemin B, Kauffmann F, Pin I, Le Moual N, Bousquet J, Gormand F, et al. Air pollution and asthma control in the epidemiological study on the Genetics and Environment of Asthma. J Epidemiol Community Health 2012;66:796-802.
8. Weinmayr G, Romeo E, De Sario M, Weiland SK, Forastiere F. Short-term effects of PM10 and NO2 on respiratory health among children with asthma or asthma-like symptoms: a systematic review and meta-analysis. Environ Health Perspect 2010;118:449-57.
9. Lee YM, Lee JH, Kim HC, Ha E. Effects of PM10 on mortality in pure COPD and asthma-COPD overlap: difference in exposure duration, gender, and smoking status. Sci Rep 2020;10:2402.
10. Wunnapuk K, Pothirat C, Manokeaw S, Phetsuk N, Chaiwong W, Phuackchantuck R, et al. PM10-related DNA damage, cytokinetic defects, and cell death in COPD patients from Chiang Dao district, Chiang Mai, Thailand. Environ Sci Pollut Res Int 2019;26:25326-40.
11. Heinrich J, Schikowski T. COPD patients as vulnerable subpopulation for exposure to ambient air pollution. Curr Environ Health Rep 2018;5:70-6.
12. Park YB, Rhee CK, Yoon HK, Oh YM, Lim SY, Lee JH, et al. Revised (2018) COPD clinical practice guideline of the Korean Academy of Tuberculosis and Respiratory Disease: a summary. Tuberc Respir Dis 2018;81:261-73.
13. Hirota JA, Gold MJ, Hiebert PR, Parkinson LG, Wee T, Smith D, et al. The nucleotide-binding domain, leucine-rich repeat protein 3 inflammasome/IL-1 receptor I axis mediates innate, but not adaptive, immune responses after exposure to particulate matter under 10 μm. Am J Respir Cell Mol Biol 2015;52:96-105.
14. Wark PA, Johnston SL, Bucchieri F, Powell R, Puddicombe S, Laza-Stanca V, et al. Asthmatic bronchial epithelial cells have a deficient innate immune response to infection with rhinovirus. J Exp Med 2005;201:937-47.
15. Kicic A, Sutanto EN, Stevens PT, Knight DA, Stick SM. Intrinsic biochemical and functional differences in bronchial epithelial cells of children with asthma. Am J Respir Crit Care Med 2006;174:1110-8.
16. Zosky GR, Boylen CE, Wong RS, Smirk MN, Gutiérrez L, Woodward RC, et al. Variability and consistency in lung inflammatory responses to particles with a geogenic origin. Respirology 2014;19:58-66.
17. Hirota JA, Hirota SA, Warner SM, Stefanowicz D, Shaheen F, Beck PL, et al. The airway epithelium nucleotide-binding domain and leucine-rich repeat protein 3 inflammasome is activated by urban particulate matter. J Allergy Clin Immunol 2012;129:1116-25.
18. Reibman J, Hsu Y, Chen LC, Bleck B, Gordon T. Airway epithelial cells release MIP-3α/CCL20 in response to cytokines and ambient particulate matter. Am J Respir Cell Mol Biol 2003;28:648-54.
19. Lee JH, Sohn JH, Ryu SY, Hong CS, Moon KD, Park JW. A novel human anti-VCAM-1 monoclonal antibody ameliorates airway inflammation and remodelling. J Cell Mol Med 2013;17:1271-81.
20. An TJ, Rhee CK, Kim JH, Lee YR, Chon JY, Park CK, et al. Effects of macrolide and corticosteroid in neutrophilic asthma mouse model. Tuberc Respir Dis 2018;81:80-7.
21. Kang JY, Kim IK, Hur J, Kim SC, Lee SY, Kwon SS, et al. Expression of muscarinic receptors and the effect of tiotropium bromide in aged mouse model of chronic asthma. Tuberc Respir Dis 2019;82:71-80.
22. Trapnell C, Pachter L, Salzberg SL. TopHat: discovering splice junctions with RNA-Seq. Bioinformatics 2009;25:1105-11.
23. Roberts A, Trapnell C, Donaghey J, Rinn JL, Pachter L. Improving RNA-Seq expression estimates by correcting for fragment bias. Genome Biol 2011;12:R22.
24. Huang KL, Liu SY, Chou CC, Lee YH, Cheng TJ. The effect of size-segregated ambient particulate matter on Th1/Th2-like immune responses in mice. PLoS One 2017;12:e0173158.
25. Miyata R, van Eeden SF. The innate and adaptive immune response induced by alveolar macrophages exposed to ambient particulate matter. Toxicol Appl Pharmacol 2011;257:209-26.
26. Zosky GR, Iosifidis T, Perks K, Ditcham WG, Devadason SG, Siah WS, et al. The concentration of iron in real-world geogenic PM(1)(0) is associated with increased inflammation and deficits in lung function in mice. PLoS One 2014;9:e90609.
27. Zhao S, Wang J, Xie Q, Luo L, Zhu Z, Liu Y, et al. Elucidating mechanisms of long-term gasoline vehicle exhaust exposure-induced erectile dysfunction in a rat model. J Sex Med 2019;16:155-67.
28. Kwon SO, Hong SH, Han YJ, Bak SH, Kim J, Lee MK, et al. Long-term exposure to PM10 and NO2 in relation to lung function and imaging phenotypes in a COPD cohort. Respir Res 2020;21:247.
29. Rue L, Banez-Coronel M, Creus-Muncunill J, Giralt A, Alcala-Vida R, Mentxaka G, et al. Targeting CAG repeat RNAs reduces Huntington's disease phenotype independently of huntingtin levels. J Clin Invest 2016;126:4319-30.
30. Kitagawa T, Taniuchi K, Tsuboi M, Sakaguchi M, Kohsaki T, Okabayashi T, et al. Circulating pancreatic cancer exosomal RNAs for detection of pancreatic cancer. Mol Oncol 2019;13:212-27.
31. Taye M, Lee W, Jeon S, Yoon J, Dessie T, Hanotte O, et al. Exploring evidence of positive selection signatures in cattle breeds selected for different traits. Mamm Genome

2017;28:528-41.
32. Cai SR, Chen CQ, Wang Z, He YL, Cui J, Wu WH, et al. Expression of phosphatase of regenerating liver-3 in gastric cancer, its relationship with prognosis, and its role in gastric cancer cell proliferation. Zhonghua Yi Xue Za Zhi 2008;88:2326-30.
33. Park J, Kim EK, Kim MA, Kim TH, Chang JH, Ryu YJ, et al. Increased risk of exacerbation in asthma predominant asthma-chronic obstructive pulmonary disease overlap syndrome. Tuberc Respir Dis 2018;81:289-98.
34. Gold MJ, Hiebert PR, Park HY, Stefanowicz D, Le A, Starkey MR, et al. Mucosal production of uric acid by airway epithelial cells contributes to particulate matter-induced allergic sensitization. Mucosal Immunol 2016;9:809-20.
35. Clifford HD, Perks KL, Zosky GR. Geogenic PM(1)(0) exposure exacerbates responses to influenza infection. Sci Total Environ 2015;533:275-82.
36. Cho YS, Oh YM. Dilemma of asthma treatment in mild patients. Tuberc Respir Dis 2019;82:190-3.
37. Heyder J. Deposition of inhaled particles in the human respiratory tract and consequences for regional targeting in respiratory drug delivery. Proc Am Thorac Soc 2004;1:315-20.
38. Parker D, Prince A. Innate immunity in the respiratory epithelium. Am J Respir Cell Mol Biol 2011;45:189-201.